The Canadian Mineralogist
Vol. 46, pp. 1465-1476 (2008)
DOI: 10.3749/canmin.46.6.1465

THE MECHANISM OF COUPLING IN THE MODULATED STRUCTURE OF NEPHELINE

ROSS J. ANGEL[§]

Crystallography Laboratory, Department of Geosciences, Virginia Tech, Blacksburg, Virginia 24060, USA

G. DIEGO GATTA

Dipartimento di Scienze della Terra, Università degli Studi di Milano, Via Botticelli 23, I–20133 Milano, Italy

TIZIANA BOFFA BALLARAN

Bayerisches Geoinstitut, Universität Bayreuth, D–95440 Bayreuth, Germany

MICHAEL A. CARPENTER

Department of Earth Sciences, University of Cambridge, Downing Street, Cambridge CB2 3EQ, UK

ABSTRACT

The crystal structures of a nepheline, $K_{0.54}Na_{3.24}Ca_{0.03}\square_{0.19}Al_{3.84}Si_{4.16}O_{16}$, and that of the same sample annealed at high temperature to induce K–vacancy disorder, have been determined at several temperatures down to 15 K by single-crystal X-ray diffraction. The largest structural change in both crystals with decreasing temperature is the decrease of the *T*1–O1–*T*2 angle, corresponding to an increase in the tilt of the *T*1 and *T*2 tetrahedra within the framework. The tetrahedra in the annealed sample have a smaller tilt than in the natural sample at any given temperature. The correlation of the tilts of the tetrahedra with changes in the intensities of satellite reflections confirms that the satellites arise from a displacive modulation of the framework of tetrahedra. Distance-least-squares simulations suggest that the modulation creates larger and smaller cavities within the extra-framework channels that contain the K atoms. Analysis of the K–O bond lengths with both the state of K–□ order and temperature indicate that the coupling between K–□ order and the framework modulation occurs through the K–O2 bond. An increase in the average K–O2 bond length with decreasing temperature or increasing K–□ order supports the modulation of the framework. Shortening of the K–O2 bond leads to rotations of the tetrahedra that are opposite to those associated with the modulation, and thus suppresses it.

Keywords: nepheline, low-temperature equilibration, incommensurate structure, X-ray diffraction, structure refinement.

SOMMAIRE

Nous avons déterminé par diffraction X sur monocristal la structure cristalline de la néphéline, $K_{0.54}Na_{3.24}Ca_{0.03}\square_{0.19}Al_{3.84}Si_{4.16}O_{16}$, et celle du même échantillon recuit à température élevée afin de provoquer un désordre entre les atomes K et les lacunes, et par la suite ré-équilibré à plusieurs degrés de refroidissement jusqu'à 15 K. L'abaissement de la température cause surtout une diminution de l'angle *T*1–O1–*T*2, ce qui correspond à une augmentation de l'inclinaison des tétraèdres *T*1 et *T*2 dans la trame. Les tétraèdres dans l'échantillon recuit montrent une inclinaison moins importante que l'échantillon naturel à une température donnée. Une corrélation des inclinaisons des tétraèdres avec les changements en intensité des réflexions satellites confirme l'hypothèse que ces satellites témoignent d'une modulation dans les déplacements de tétraèdres dans la trame. Une simulation par distance-moindres-carrés montre que la modulation crée des cavités plus et moins volumineuses dans les sites externes à la trame, où logent les atomes de potassium. Une analyse des longueurs des liaisons K–O en fonction du degré d'ordre K–□ et de la température indique un couplage entre le degré d'ordre K–□ et la modulation de la trame par le biais de la liaison K–O2. Une augmentation de la longueur moyenne de la liaison K–O2 à mesure que diminue la température ou qu'augmente le degré d'ordre K–□ provoque la modulation de la trame. En revanche, une diminution de la longueur de la liaison K–O2 mène à une rotation des tétraèdres opposée à celle que cause la modulation, et donc l'atténue.

(Traduit par la Rédaction)

Mots-clés: néphéline, ré-équilibrage à faible température, structure incommensurable, diffraction X, affinement de la structure.

§ *E-mail address*: rangel@vt.edu

Introduction

The difficulty in determining the structural origin of the satellite reflections in nepheline, $(K,Na,Ca,\square)_4Al_{4-x}Si_{4+x}O_{16}$, has arisen from both their incommensurate nature and their intrinsic weakness, making reliable measurements of a significant number of satellite intensities difficult. Also challenging for models of the ordering in terms of an ordered commensurate supercell is the sheer size of the supercell and thus the large number of degrees of freedom in any model. In this contribution, we take an alternative approach. We correlate the changes in the average structure of nepheline, easily determined from the Bragg reflections alone, with the qualitative changes in the satellite intensities. In particular, our measurements were performed below room temperature so that no changes in the state of K–vacancy (K–□) order occur during the measurements, in contrast to structure determinations at elevated temperatures (Foreman & Peacor 1970). On the other hand, complete K–□ disorder can be induced by annealing the samples at modest temperatures (McConnell 1981, Hayward *et al.* 2000) and then quenching in this state of disorder prior to diffraction measurements. This approach allows us to confirm the conclusion of previous investigators (Parker & McConnell 1971, McConnell 1981, 1991) that a major contribution to the satellite intensities comes from modulation of the framework and, for the first time, to identify the atomic-scale mechanism of coupling between the modulation of the framework and K–□ order in the channels.

Background

The structure of nepheline is comprised of corner-linked SiO_4 and AlO_4 tetrahedra that form a fully connected three-dimensional framework with the same topology as that of tridymite, SiO_2 (Buerger *et al.* 1954, Hahn & Buerger 1954; Fig. 1). The "topological symmetry" (Baerlocher *et al.* 2001) of the idealized framework of nepheline is $P6_3/mmc$. The ordered distribution of Al and Si in the framework reduces the symmetry to $P6_3$. The net negative charge of the framework is charge-balanced by alkali cations that occupy two channels parallel to [001] within the framework, to give an ideal formula of $KNa_3Al_4Si_4O_{16}$, with Z = 2. With this composition, the larger channel with trigonal symmetry is fully occupied by K, whereas the smaller distorted channel is fully occupied by Na. Some substitution of Na for K typically leads to excess Na, which is located in the trigonal channel. A small excess of Si over Al (*e.g.*, Smith & Sahama 1954) and replacement of Na by Ca are charge-balanced by vacancies in this trigonal channel.

The abiding interest in nepheline arises from the presence of satellite reflections in the diffraction patterns from some nepheline crystals in addition to the Bragg reflections. The origin of these satellites has been debated since their first observation by X-ray diffraction (Sahama 1958) and electron diffraction (McConnell 1962). The satellites occur at positions $\pm(^1/_3, ^1/_3, z^*)$ with $z^* \approx 0.20$ (Fig. 2). Although the value of z^* is incommensurate, these additional reflections must arise from ordering in the structure in a hexagonal supercell with approximate dimensions $\sqrt{3}a$ and $5c$, where the unit-cell parameters a and c of the average structure are approximately 10 and 8.7 Å, respectively. The early suggestion (McConnell 1962) that the satellites may arise from additional ordering of Al and Si among the tetrahedral sites, or from domains of different Al–Si order, has been excluded by NMR measurements (Stebbins *et al.* 1986, Hovis *et al.* 1992), X-ray structure refinements (Foreman & Peacor 1970, Dollase & Peacor 1971, Gregorkiewitz 1984, Hassan *et al.* 2003, Tait *et al.* 2003), and the failure to observe corresponding domain structures by TEM (*e.g.*, Hassan *et al.* 2003). The remaining possibilities are that the satellite reflections result from either a purely displacive modulation of the framework (*i.e.*, by organized tilts of the tetrahedra), or from ordering of cations and vacancies in the partially occupied trigonal channels. An attempt by Parker (1972) to explain the diffraction effects in terms of a domain model for the framework displacements was not convincing, whereas Patterson maps calculated from the intensities of the satellite reflections cannot be explained by ordering of cations and vacancies in the extra-framework channels alone (Parker & McConnell 1971, 1991). Experimental and theoretical evidence now points to both mechanisms playing a role in the stabilization of the modulated structure (Parker 1970, Simmons & Peacor 1972, McConnell 1981, McConnell 1991, Hassan *et al.* 2003, Gatta & Angel 2007). In particular, Hayward *et al.* (2000) showed by computer simulation that the nepheline framework, in the absence of extra-framework cations, has an intrinsic instability that leads to a modulation of the tilts of the tetrahedra with a wave vector that approximates that of the observed position of the satellites.

Experimental

The nepheline sample used in these experiments was taken from the Harker mineral collection of the University of Cambridge, specimen 65984, and comes from the intrusive aplite of Snipe River, Tambani, Malawi. The K, Na and Ca content was determined by wet-chemical analysis (McConnell 1962), and the composition is $K_{0.54}Na_{3.24}Ca_{0.03}\square_{0.19}Al_{3.84}Si_{4.16}O_{16}$, with the Al/Si value determined by charge balance. The specimen is unusual in that X-ray and electron-diffraction measurements (McConnell 1962, 1981) showed that it has the sharpest and strongest satellite reflections of any sample of nepheline studied. We determined that room-temperature X-ray-diffraction studies of a number of crystals from this sample yield the same refined structure, bond lengths and angles within mutual standard deviations. In

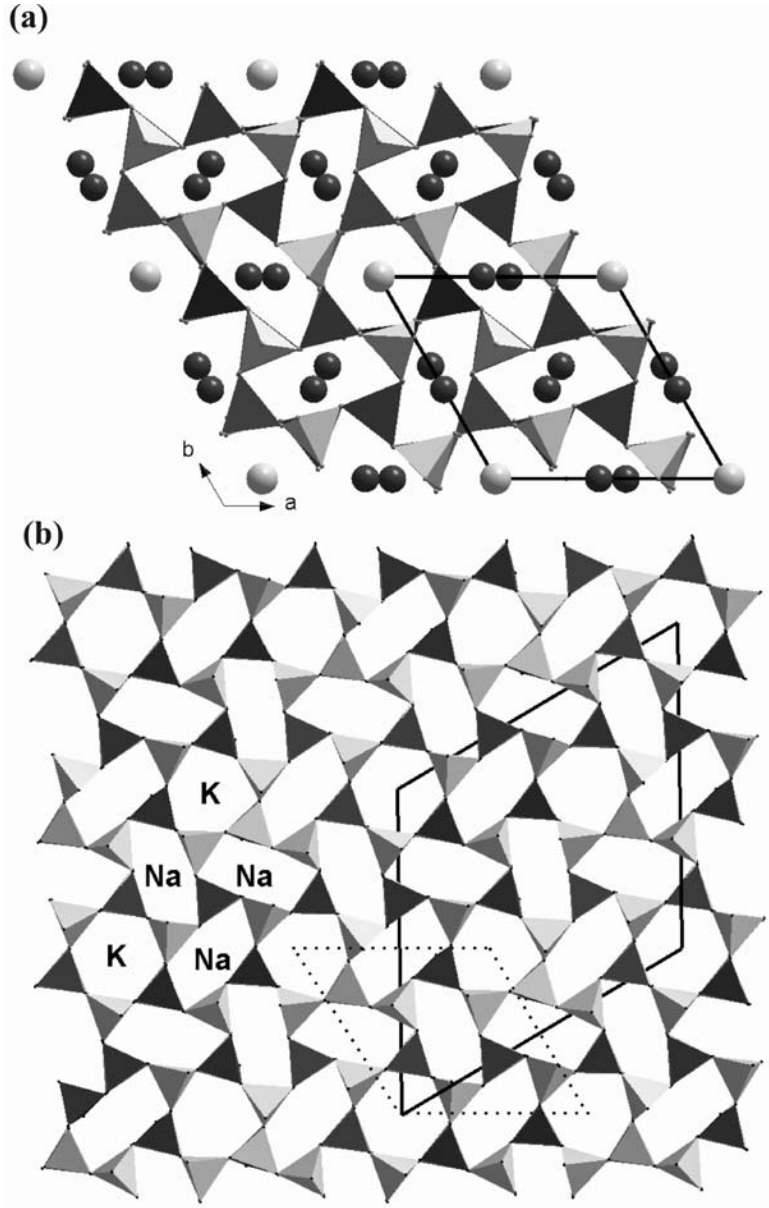

FIG. 1. (*a*) The average structure of nepheline viewed down [001]. The Si-dominant tetrahedra are represented in gray, and the Al-dominant tetrahedra, in black. Large gray spheres represent the K sites, located in the regular six-membered ring channels, whereas the small black spheres represent the Na sites located in the elliptically distorted six-membered ring channels. (*b*) DLS structural model of the framework of tetrahedra in nepheline. The heavy lines indicate the unit cell with the lattice parameters $\sqrt{3}a$, c, and the dotted lines, the unit cell of the average structure. Note the increased distortion of both the Na channels and $^2/_3$ of the K channels.

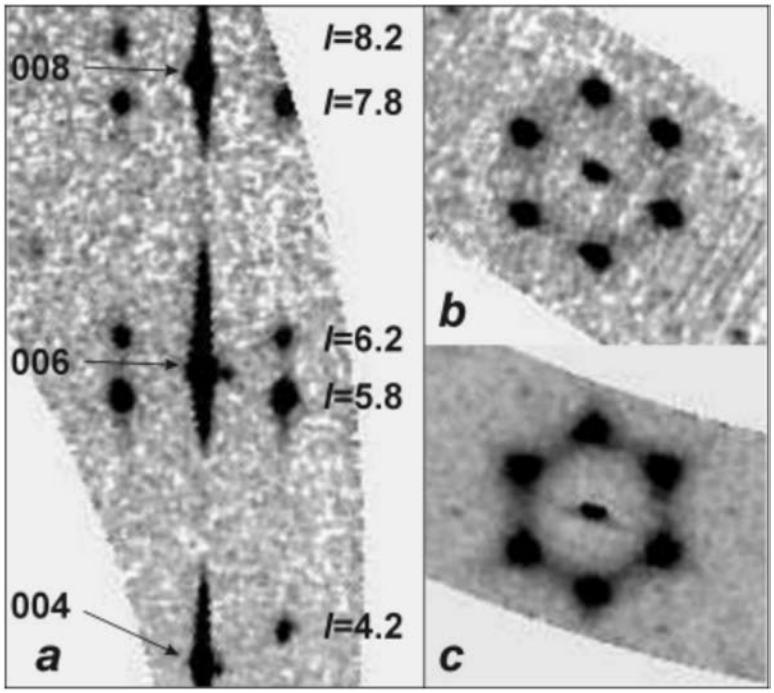

FIG. 2. Reciprocal lattice sections of nepheline reconstructed from single-crystal X-ray-diffraction datasets collected by CCD. (a) The section containing c^* (vertical) and 110* (horizontal) shows the Bragg spots $00l$ (l = odd are absent owing to the 6_3 symmetry axis) and satellites at levels of $l \pm 0.2$. (b) The section at $l = 5.8$ of the natural sample, showing the six satellites at $h,k = \pm(^1/_3, ^1/_3)$ group around the 0,0,5.8 position. The central spot is the white-beam tail from the 006 Bragg reflection. (c) The $l = 5.8$ section of the annealed sample shows additional diffuse streaks between the satellites that indicate a lower correlation of the structural modulation compared to the well-ordered natural sample.

this study, we measured the structure of a crystal from this sample, and also of crystals annealed to induce K–□ disorder within the extra-framework channels.

Two different procedures were applied to anneal the nepheline, each of which should have been sufficient to completely disorder the K and vacancies (McConnell 1981). The crystal measured at 15 K was annealed at 300°C for 3 hours, approximately 6 months prior to the X-ray-diffraction study. Another portion of this annealed sample was annealed a second time, at 390°C for 2.5 hours, and measured within a period of four days in a series of measurements down to 100 K.

The low-temperature intensity data were collected on an Oxford Diffraction Xcalibur diffractometer equipped with Mo radiation, ENHANCE™ X-ray optics, and a Sapphire III™ CCD detector. For measurements down to 100 K, the crystals were cooled with a CRYOJET™ open-flow nitrogen system with a temperature stability of better than 0.2 K, and an absolute uncertainty in temperature at the crystal position of <2 K. For each crystal, the data collections were performed in a single cooling and heating cycle from room temperature down to 100 K and then back to room temperature. Some datasets were collected on the cooling leg of the cycle, and some on the heating leg (Table 1); in either case, the crystal was held at the target temperature for at least 30 minutes prior to the start of the data collection. The 15 K data were obtained with a HELIJET™ open-flow helium system with a temperature stability of better than 0.2 K, and a temperature uncertainty at the crystal position of <3 K.

Data were collected over a full sphere of reciprocal space out to $2\theta = 60°$, except for the 15 K data, which covered a half sphere to $2\theta = 60°$. Cell parameters were determined from reflection positions harvested from the CCD dataset. Data collection and reduction were performed with the CRYSALIS™ software supplied by Oxford Diffraction, including an absorption correction by Gaussian integration based upon the physical description of the crystal. Structure refinements were

performed with WIN–GX (Farrugia 1999) and SHELX–L (Sheldrick 2008) using squared structure-factors. There was no evidence of any symmetry change from the $P6_3$ space group reported previously for the average structure of nepheline at room or elevated temperatures, and the Flack parameter refined to zero within 1.5 *esd* for all datasets. Extensive testing showed that the results of the structure refinements are not sensitive to the Al–Si distribution imposed on the model, provided that the alternation of Al-rich and Si-rich tetrahedra is maintained. This is to be expected, as Al and Si have very similar X-ray scattering factors. The refinements reported here were therefore performed with the *T*2 and *T*3 sites fully occupied by Si, and the *T*1 and *T*4 sites fully occupied by Al. Final refinement-parameters, structural parameters, and selected bond-lengths and angles are reported in Tables 1–4. Crystallographic data have been deposited with the ICSD under CSD numbers 418442–418449 inclusive. These may be obtained from Fachinformationszentrum Karlsruhe; e-mail: crysdata@fiz-karlsruhe.de, http://www.fiz-karlsruhe.de/request_for_deposited_data.html) on quoting the CSD numbers.

Simulations of the structure of nepheline were performed using the DLS–76 program (Baerlocher *et al.* 1977), in which the AlO_4 and SiO_4 tetrahedra were constrained to be ideal, with bond lengths of Al–O = 1.74 Å and Si–O = 1.62 Å. The five-fold supercell corresponding to the $z^* \approx 0.2$ of the satellites allows too many degrees of freedom for a stable simulation. Therefore, simulations were performed with the $\sqrt{3}a$, c supercell constrained to the $P6_3$ symmetry that would hold were the satellites to occur at position $z^* = 0$, rather than the observed $z^* \approx 0.2$. It has previously been argued that such a model represents an average of the true modulated structure projected into the smaller $\sqrt{3}a$, c supercell (Parker & McConnell 1971, McConnell 1991), or at least the component of the ordering patterns that includes the displacement of the O1 atoms (McConnell 1991). Although this cannot be quite correct, as the RUM simulations (Hayward *et al.* 2000) show that the [110]* direction is a different soft-phonon branch from the two branches contributing to the satellites at $z^* \sim 0.2$, the results of the simulations in the smaller supercell do provide some insights into possible mechanisms for the development of the modulation.

RESULTS

The refined structure of the untreated crystal at room temperature is very similar to the recently published structures of nepheline (*e.g.*, Gregorkiewitz 1984, Hassan *et al.* 2003, Tait *et al.* 2003). It has been previously argued (*e.g.*, Stebbins *et al.* 1986, Hassan *et al.* 2003, Tait *et al.* 2003) that natural nepheline possesses the maximum degree of Al–Si order possible, with effectively strict alternation of Al and Si tetrahedra through the framework. Further, the mean <*T*–O> bond lengths of each tetrahedron do not change significantly upon cooling the crystals below room temperature, and

TABLE 1. CRYSTAL DATA AND STRUCTURE-REFINEMENT INFORMATION ON NEPHELINE

Sample		Natural	Natural	Natural	Annealed	Annealed	Annealed	Annealed	Annealed
Temperature (K)		290(2) K	200(2) K	110(2) K	298(2) K	220(2) K	150(2) K	100(2) K	15(2) K
Unit-cell parameters									
a (Å)		9.9995(5)	9.9890(5)	9.9820(5)	9.9861(6)	9.9751(7)	9.9698(7)	9.9685(6)	9.9801(5)
c (Å)		8.3766(6)	8.3687(6)	8.3670(6)	8.3697(5)	8.3658(6)	8.3615(6)	8.3608(5)	8.3707(7)
V (Å^3)		725.36(7)	723.16(7)	722.00(7)	722.82(8)	720.90(9)	719.76(9)	719.51(7)	722.04(8)
Absorption coefficient (mm^{-1})		1.123	1.127	1.129	1.127	1.130	1.132	1.132	1.128
Reflections collected		14710	14651	14582	14948	13185	13556	13463	7594
Independent reflections		1410	1405	1397	1398	1397	1393	1394	1330
[R(int)]		0.0465	0.0478	0.0517	0.0251	0.0249	0.0255	0.0256	0.0211
Completeness to θ = 30° (%)		99.6	99.6	99.6	99.6	99.7	99.5	99.6	99.7
Absorption correction		Analytical	Analytical	Analytical	Analytical	Analytical	Analytical	Analytical	Semi-emp.*
Max. and min. transmission		0.870, 0.738	0.870, 0.738	0.870, 0.738	0.870, 0.738	0.875, 0.709	0.887, 0.709	0.887, 0.709	0.7398, 0.702
Data / restraints / parameters		1410/1/91	1405/1/91	1397/1/91	1398/1/91	1397/1/91	1393/1/91	1394/1/91	1330/1/91
Goodness-of-fit on F^2		1.062	1.085	1.125	1.090	1.059	1.110	1.103	1.124
Final R indices	R1	0.0329	0.0332	0.0337	0.0244	0.0244	0.0248	0.0264	0.0450
[I > 2σ(I)]	wR2	0.0952	0.0930	0.0959	0.0745	0.0760	0.0727	0.0745	0.1319
R indices (all data)	R1	0.0337	0.0338	0.0342	0.0245	0.0245	0.0249	0.0265	0.0479
	wR2	0.0961	0.0936	0.0967	0.0746	0.0762	0.0729	0.0746	0.1355
Flack parameter		0.14(18)	0.21(18)	0.12(19)	0.04(14)	0.03(13)	0.00(16)	0.02(17)	0.32(17)
Largest diffraction peak		0.610	0.541	0.553	0.437	0.424	0.478	0.545	1.782
and hole (e•Å^{-3})		-0.511	-0.523	-0.603	-0.746	-0.780	-0.816	-0.867	-0.658

* Semi-empirical, from equivalents.

TABLE 2. COORDINATES AND EQUIVALENT ISOTROPIC DISPLACEMENT PARAMETERS (Å^2) OF ATOMS IN NEPHELINE

	x	*y*	*z*	*U*(eq)		*x*	*y*	*z*	*U*(eq)
	Annealed sample, 220 K					**Natural sample, 290 K**			
K	0	0	0.0031(3)	0.028(1)	K	0	0	0.0037(4)	0.033(1)
Na	0.5547(1)	0.9979(1)	0.5081(2)	0.020(1)	Na	0.5541(1)	0.9972(1)	0.5080(3)	0.025(1)
T(1)	⅔	⅓	0.7017(1)	0.011(1)	*T*(1)	⅔	⅓	0.7015(2)	0.013(1)
T(2)	⅔	⅓	0.3124(1)	0.012(1)	*T*(2)	⅔	⅓	0.3132(2)	0.014(1)
T(3)	0.9066(1)	0.6664(1)	0.8226(1)	0.011(1)	*T*(3)	0.9057(1)	0.6661(1)	0.8224(1)	0.014(1)
T(4)	0.9071(1)	0.6679(1)	0.1958(1)	0.010(1)	*T*(4)	0.9064(1)	0.6676(1)	0.1959(1)	0.012(1)
O(1)	0.6640(20)	0.2910(11)	0.5023(8)	0.028(1)	O(1)	0.6620(20)	0.2891(13)	0.5013(11)	0.033(2)
O(2)	0.9743(2)	0.6842(2)	0.0022(3)	0.028(1)	O(2)	0.9729(2)	0.6835(3)	0.0027(5)	0.034(1)
O(3)	0.8272(2)	0.4773(2)	0.2512(4)	0.033(1)	O(3)	0.8265(3)	0.4775(3)	0.2514(6)	0.038(1)
O(4)	0.8373(2)	0.4896(2)	0.7645(4)	0.029(1)	O(4)	0.8367(3)	0.4898(3)	0.7642(6)	0.034(1)
O(5)	0.7739(2)	0.7145(2)	0.8252(3)	0.016(1)	O(5)	0.7737(3)	0.7147(3)	0.8241(4)	0.020(1)
O(6)	0.7767(2)	0.7335(2)	0.2007(3)	0.018(1)	O(6)	0.7760(3)	0.7329(3)	0.2011(4)	0.023(1)
	Annealed sample, 150 K					**Natural sample, 200 K**			
K	0	0	0.0029(3)	0.024(1)	K	0	0	0.0034(4)	0.028(1)
Na	0.5550(1)	0.9978(1)	0.5082(3)	0.017(1)	Na	0.5545(1)	0.9972(1)	0.5081(3)	0.021(1)
T(1)	⅔	⅓	0.7017(1)	0.010(1)	*T*(1)	⅔	⅓	0.7014(2)	0.012(1)
T(2)	⅔	⅓	0.3124(1)	0.011(1)	*T*(2)	⅔	⅓	0.3134(2)	0.013(1)
T(3)	0.9067(1)	0.6662(1)	0.8226(1)	0.010(1)	*T*(3)	0.9061(1)	0.6660(1)	0.8223(1)	0.013(1)
T(4)	0.9073(1)	0.6677(1)	0.1958(1)	0.009(1)	*T*(4)	0.9068(1)	0.6675(1)	0.1959(1)	0.011(1)
O(1)	0.6623(15)	0.2875(9)	0.5015(10)	0.024(1)	O(1)	0.6620(16)	0.2858(9)	0.5015(12)	0.028(1)
O(2)	0.9745(2)	0.6837(2)	0.0023(4)	0.028(1)	O(2)	0.9734(2)	0.6830(3)	0.0027(5)	0.033(1)
O(3)	0.8273(3)	0.4771(3)	0.2517(5)	0.033(1)	O(3)	0.8269(3)	0.4775(3)	0.2516(6)	0.037(1)
O(4)	0.8377(3)	0.4894(3)	0.7635(5)	0.029(1)	O(4)	0.8373(3)	0.4896(3)	0.7629(6)	0.033(1)
O(5)	0.7739(2)	0.7143(2)	0.8255(3)	0.014(1)	O(5)	0.7736(3)	0.7145(3)	0.8249(4)	0.018(1)
O(6)	0.7767(2)	0.7333(2)	0.2008(4)	0.016(1)	O(6)	0.7765(3)	0.7330(3)	0.2011(5)	0.021(1)
	Annealed sample, 100 K					**Natural sample, 110 K**			
K	0	0	0.0028(4)	0.022(1)	K	0	0	0.0031(4)	0.024(1)
Na	0.5551(1)	0.9976(1)	0.5085(3)	0.015(1)	Na	0.5547(1)	0.9971(1)	0.5082(3)	0.017(1)
T(1)	⅔	⅓	0.7017(1)	0.009(1)	*T*(1)	⅔	⅓	0.7014(2)	0.010(1)
T(2)	⅔	⅓	0.3124(1)	0.010(1)	*T*(2)	⅔	⅓	0.3137(2)	0.012(1)
T(3)	0.9067(1)	0.6661(1)	0.8225(1)	0.010(1)	*T*(3)	0.9064(1)	0.6660(1)	0.8222(1)	0.012(1)
T(4)	0.9074(1)	0.6675(1)	0.1958(1)	0.008(1)	*T*(4)	0.9071(1)	0.6672(1)	0.1959(1)	0.010(1)
O(1)	0.6605(12)	0.2846(7)	0.5008(11)	0.021(1)	O(1)	0.6611(12)	0.2825(8)	0.5005(12)	0.024(1)
O(2)	0.9743(2)	0.6830(2)	0.0023(5)	0.029(1)	O(2)	0.9734(2)	0.6822(3)	0.0022(5)	0.034(1)
O(3)	0.8273(3)	0.4771(3)	0.2518(6)	0.033(1)	O(3)	0.8270(4)	0.4774(3)	0.2518(7)	0.038(1)
O(4)	0.8379(3)	0.4894(3)	0.7624(6)	0.029(1)	O(4)	0.8374(4)	0.4891(3)	0.7613(6)	0.032(1)
O(5)	0.7736(3)	0.7141(2)	0.8257(4)	0.014(1)	O(5)	0.7736(3)	0.7143(3)	0.8253(4)	0.016(1)
O(6)	0.7769(3)	0.7333(2)	0.2011(4)	0.015(1)	O(6)	0.7765(3)	0.7329(3)	0.2012(5)	0.018(1)
	Annealed sample, 15 K					**Annealed sample, 298 K**			
K	0	0	0.0037(4)	0.022(1)	K	0	0	0.0030(3)	0.032(1)
Na	0.5554(1)	0.9976(1)	0.5086(4)	0.017(1)	Na	0.5545(1)	0.9980(1)	0.5080(2)	0.024(1)
T(1)	⅔	⅓	0.7010(2)	0.012(1)	*T*(1)	⅔	⅓	0.7018(1)	0.012(1)
T(2)	⅔	⅓	0.3136(2)	0.014(1)	*T*(2)	⅔	⅓	0.3123(1)	0.013(1)
T(3)	0.9067(1)	0.6658(1)	0.8222(1)	0.014(1)	*T*(3)	0.9063(1)	0.6665(1)	0.8226(1)	0.012(1)
T(4)	0.9073(1)	0.6671(1)	0.1961(1)	0.012(1)	*T*(4)	0.9067(1)	0.6680(1)	0.1959(1)	0.010(1)
O(1)	0.6602(11)	0.2797(8)	0.5053(15)	0.023(1)	O(1)	0.6660(30)	0.2950(17)	0.5021(8)	0.030(2)
O(2)	0.9732(2)	0.6814(3)	0.0034(6)	0.035(1)	O(2)	0.9739(2)	0.6845(2)	0.0022(3)	0.028(1)
O(3)	0.8287(4)	0.4781(4)	0.2515(8)	0.038(1)	O(3)	0.8267(2)	0.4773(2)	0.2508(4)	0.033(1)
O(4)	0.8365(5)	0.4889(4)	0.7610(7)	0.034(1)	O(4)	0.8371(2)	0.4898(2)	0.7651(4)	0.030(1)
O(5)	0.7746(3)	0.7152(4)	0.8251(5)	0.019(1)	O(5)	0.7739(2)	0.7148(2)	0.8246(3)	0.018(1)
O(6)	0.7762(3)	0.7315(3)	0.2007(6)	0.020(1)	O(6)	0.7764(2)	0.7334(2)	0.2008(3)	0.021(1)

U(eq) is defined as one third of the trace of the orthogonalized U^{ij} tensor. Note: The K site was modeled with occupancy of 0.57K and 0.24Na to represent the occupancy of 0.24Na + 0.54K + 0.03Ca deduced from the results of the chemical analysis (McConnell 1962).

there are no significant differences between those of the annealed sample and those of the natural starting material. Therefore, we make the reasonable assumption that neither the annealing process nor the cooling changed the state of Al–Si order. All of the changes in structural parameters that occur upon cooling of a particular crystal are completely reversible (within the uncertainties of the structure refinements) upon returning the crystal to higher temperatures. They must therefore represent structural changes with little or no activation energies, which are thus displacive, rather than reconstructive, in character.

The one significant difference between the previous refinements of the structure and those reported here is the value of the *T*1–O1–*T*2 angle. In our untreated sample, this is 151.0(3)° at 290 K, which is some 1.5° – 5.5° smaller than found in previous refinements (*e.g.*, Gregorkiewitz 1984, Hassan *et al.* 2003, Tait *et al.* 2003). At room temperature, the same angle in the annealed sample is 153.7(3)°. These large differences in this one angle do not arise from the choice of model for the channel sites. Test refinements show that freely refining (or varying over a wide range) the occupancies of one or both of the channel sites changes the value of the *T*1–O1–*T*2 angle by no more than 0.1°. Similarly, variations in data-collection procedures (such as collecting a hemisphere rather than a sphere of data) and data-reduction algorithms change this angle by less than one *esd*. Part of these differences could arise from the >90% correlation between the fractional coor-

dinates of the O1 atom and its anisotropic displacement parameters, although the modern datasets (Gregorkiewitz 1984, Hassan *et al*. 2003, Tait *et al*. 2003) all give remarkably similar values for the latter. Further, the *rms* displacements of the O1 atom calculated from the refined displacement-parameters show a smooth and reasonable decrease with temperature in both the annealed and natural samples. We therefore believe that the differences in *T*1–O1–*T*2 angles are real, and provide the key to understanding the structural evolution of nepheline at low temperature.

In interpreting the structural changes that we report here, one must remember that the structures obtained by refinement to the Bragg reflections alone represent an

TABLE 3. BOND LENGTHS [Å] OF NATURAL AND ANNEALED NEPHELINE

	Natural			Annealed				
	290 K	200 K	110 K	298 K	220 K	150 K	100 K	15 K
K-O(6) #1	2.984(3)	2.980(3)	2.981(3)	2.978(3)	2.974(2)	2.974(3)	2.975(3)	2.984(4)
K-O(5) #6	3.011(3)	3.005(3)	3.002(3)	3.002(2)	2.998(2)	2.996(3)	2.996(3)	2.997(4)
K-O(2) #2	3.039(2)	3.042(2)	3.049(2)	3.0289(16)	3.0300(16)	3.0346(18)	3.040(2)	3.055(3)
Na-O(5) #7	2.484(3)	2.474(3)	2.468(4)	2.481(2)	2.474(2)	2.468(3)	2.464(3)	2.477(4)
Na-O(2) #8	2.534(2)	2.528(2)	2.521(3)	2.5360(17)	2.5306(17)	2.5261(19)	2.523(2)	2.518(3)
Na-O(1) #9	2.557(8)	2.525(7)	2.495(6)	2.595(12)	2.560(8)	2.530(6)	2.507(5)	2.466(6)
Na-O(6) #10	2.587(4)	2.573(5)	2.560(6)	2.587(3)	2.583(2)	2.579(3)	2.578(3)	2.568(4)
Na-O(4) #11	2.588(5)	2.585(4)	2.580(4)	2.586(4)	2.579(4)	2.568(4)	2.558(5)	2.557(7)
Na-O(3) #11	2.638(5)	2.632(6)	2.631(6)	2.634(4)	2.629(4)	2.625(5)	2.626(5)	2.625(7)
Na-O(4) #12	2.778(5)	2.780(5)	2.787(5)	2.770(3)	2.771(3)	2.774(4)	2.781(5)	2.801(6)
Na-O(3) #8	2.788(5)	2.785(5)	2.784(5)	2.783(4)	2.780(3)	2.781(4)	2.780(5)	2.776(6)
T(1)-O(4)	1.719(3)	1.716(3)	1.710(3)	1.714(7)	1.718(7)	1.716(3)	1.714(3)	1.704(4)
T(1)-O(1)	1.729(10)	1.733(10)	1.749(11)	1.720(2)	1.717(2)	1.729(8)	1.739(9)	1.714(12)
T(2)-O(3)	1.612(3)	1.612(3)	1.611(3)	1.609(2)	1.609(2)	1.607(3)	1.608(3)	1.624(4)
T(2)-O(1)	1.631(10)	1.638(10)	1.635(11)	1.634(7)	1.640(7)	1.637(8)	1.635(9)	1.683(13)
T(3)-O(4)	1.615(3)	1.617(3)	1.615(3)	1.614(2)	1.615(2)	1.614(2)	1.614(3)	1.621(4)
T(3)-O(6) #16	1.618(3)	1.617(3)	1.621(2)	1.616(2)	1.615(2)	1.616(3)	1.618(3)	1.622(3)
T(3)-O(5)	1.619(2)	1.620(2)	1.623(4)	1.6181(18)	1.620(3)	1.619(2)	1.620(2)	1.623(4)
T(3)-O(2) #17	1.627(4)	1.626(4)	1.624(3)	1.621(3)	1.6181(17)	1.621(3)	1.621(4)	1.631(5)
T(4)-O(3)	1.717(3)	1.715(3)	1.713(3)	1.719(2)	1.717(2)	1.718(3)	1.716(3)	1.705(4)
T(4)-O(2)	1.726(4)	1.726(4)	1.727(2)	1.7231(18)	1.7244(17)	1.725(2)	1.725(2)	1.721(5)
T(4)-O(6)	1.726(2)	1.726(2)	1.728(4)	1.728(2)	1.729(3)	1.728(3)	1.727(4)	1.724(3)
T(4)-O(5) #20	1.729(3)	1.730(3)	1.731(3)	1.730(3)	1.730(2)	1.730(2)	1.731(3)	1.730(4)

Symmetry transformations used to generate equivalent atoms: #1: --x+y, -x+1, z; #2: --y+1, x–y, z; #3: x–1, y–1, z; #4: x–1, y–1, z–1; #5: –x+y, –x+1, z–1; #6: –y+1, x–y, z–1; #7: y, –x+y+1, z–½; #8: x–y, x, z+½; #9: x, y+1, z; #10: y, –x+y+1, z+½; #11: –x+y+1, –x+2, z; #12: x–y, x, z–½; #13: –x+y+1, –x+1, z; #14: x, y–1, z; #15: –y+2, x–y+1, z; #16: x–y+1, x, z+½; #17: x, y, z+1; #18: y,–x+y,z+½; #19: x+1, y+1, z+1; #20: x–y+1, x, z–½; #21: y, –x+y, z–½; #22: x+1, y+1, z; #23: –x+1, –y+1, z+½; #24: x, y, z–1.

TABLE 4. *T*–O–*T* ANGLES [°] IN NATURAL AND ANNEALED NEPHELINE

	Natural			Annealed				
	290 K	200 K	110 K	298 K	220 K	150 K	100 K	15 K
T(2)-O(1)-*T*(1)	151.0(3)	148.8(3)	146.9(3)	153.7(3)	151.8(3)	149.9(3)	148.5(3)	145.3(3)
T(3)#24-O(2)-*T*(4)	137.83(10)	137.70(11)	137.73(11)	137.58(8)	137.51(8)	137.44(9)	137.50(10)	137.98(13)
T(2)-O(3)-*T*(4)	141.43(19)	141.3(2)	141.3(2)	141.20(15)	141.05(15)	141.02(18)	141.1(2)	140.7(3)
T(3)-O(4)-*T*(1)	140.75(19)	140.4(2)	140.2(2)	140.64(15)	140.58(15)	140.34(18)	140.2(2)	140.9(3)
T(3)-O(5)-*T*(4)#10	141.0(2)	140.6(2)	140.3(3)	140.76(17)	140.42(16)	140.27(19)	140.1(2)	140.5(3)
T(3)#7-O(6)-*T*(4)	141.8(2)	141.8(3)	141.9(3)	141.45(17)	141.36(17)	141.4(2)	141.6(2)	141.7(3)

"average" of a more complex modulated structure that involves tilting of the tetrahedra within the framework. The strongest indication of these tilts in the average structure is the shift of the O1 oxygen atom off the triad axis at $^{2}/_{3}$ $^{1}/_{3}$ z to a general position with a formal average occupancy of $^{1}/_{3}$. The driving force for this shift of the O1 atom is the reduction of the *T*1–O1–*T*2 angle from an apparent value of 180° to ~150°. Because the *T*1 and *T*2 tetrahedra occupy sites of point symmetry 3, their bases must, on average, remain parallel to (001). The tilts of these tetrahedra then appear in the average structure as an increase in the elongation of the displacement ellipsoids of the O3 and O4 atoms that form the respective bases of the *T*1 and *T*2 tetrahedra (Dollase 1970, Gregorkiewitz 1984, Tait *et al.* 2003, Gatta & Angel 2007, and Fig. 3). This interpretation is now reinforced by our observation that these displacement ellipsoids are larger in the natural sample, which has a smaller *T*1–O1–*T*2 angle and thus a greater degree of tetrahedron tilt = ½[180° – (*T*1–O1–*T*2)] than in the annealed samples (Fig. 4b).

As temperature is decreased, the largest change in the structure of both samples is the decrease in the *T*1–O1–*T*2 bond angle caused by an increase in the shift of the O1 site from the triad axis. The shift of the O1 atom therefore results in apparent changes in the O1–*T*1–O4 and O1–*T*2–O3 angles to their respective basal atoms of oxygen. However, the increase in the *rms* displacements subparallel to [001] of these two oxygen atoms with decreasing temperature (Fig. 4a) clearly indicates that these apparent angular changes in the *T*1 and *T*2 tetrahedra are merely artifacts of averaging and, in the true local structure, the tilts of the tetrahedra increase as temperature decreases (Fig. 4b). Other changes in the framework of tetrahedra with temperature, whether O–*T*–O or *T*–O–*T* angles, are small, and their exact interpretation in terms of tilting is obscured by the nature of the averaging inherent in this refinement.

The [001] channels at $x = ½$, $y = 0$ (and equivalents) have two-fold symmetry in projection down [001] as a result of the 2_1 symmetry axis (Fig. 1). The symmetry allows the channel to be elliptically distorted by the tilting of tetrahedra and thus to better accommodate the small Na cation that occupies the channel. The change in the position of the O1 atom with temperature results

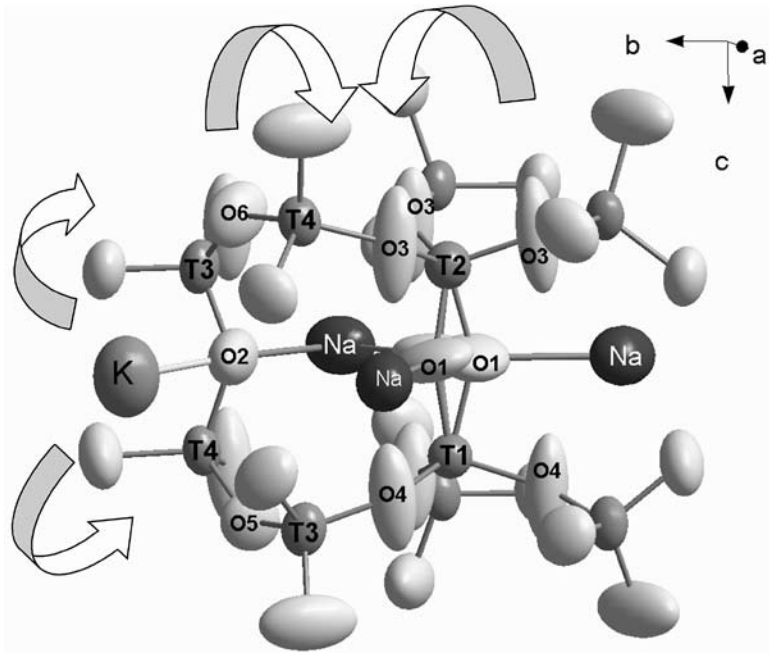

FIG. 3. A plot of the thermal ellipsoids (drawn at the 99% probability level) of the atoms in a portion of the average structure of nepheline. Note the split of the O1 oxygen atom; also, note that the displacement ellipsoids of the O3 and O4 atoms are elongate subparallel to [001], indicating that the *T*1 and *T*2 tetrahedra are locally tilted. As K and vacancies are disordered, the K–O2 bond length becomes shorter, imposing a rotation on the *T*3 and *T*4 tetrahedra indicated by the arrows, which in turn reduces the tilts of the *T*1 and *T*2 tetrahedra and increases the average *T*1–O1–*T*2 angle, and thus opposes the rotation locally required by the framework modulation.

in the largest change to either of the extra-framework cation sites in the channels, with a strong decrease in the Na–O1 distance (Fig. 5). Bearing in mind that each O1 atom is surrounded by three channels containing Na atoms, only one third of the Na sites are actually bonded to a displaced O1 oxygen and are eight-coordinated, while the remainder have no Na–O1 bond (Tait *et al*. 2003). The remaining Na–O distances all decrease by 0.01–0.02 Å between room temperature and 100 K in both the annealed and natural samples (Fig. 5). The K atom occupies a site in the larger channels at $x = 0$, $y = 0$ with site symmetry 3, and is coordinated by three symmetry-equivalent sets of three oxygen atoms at distances between 2.98 and 3.04 Å at room temperature, to provide a coordination number of nine. The shorter distances decrease with decreasing temperature in both the natural and annealed samples, but the longest distance increases with decreasing temperature (Fig. 6).

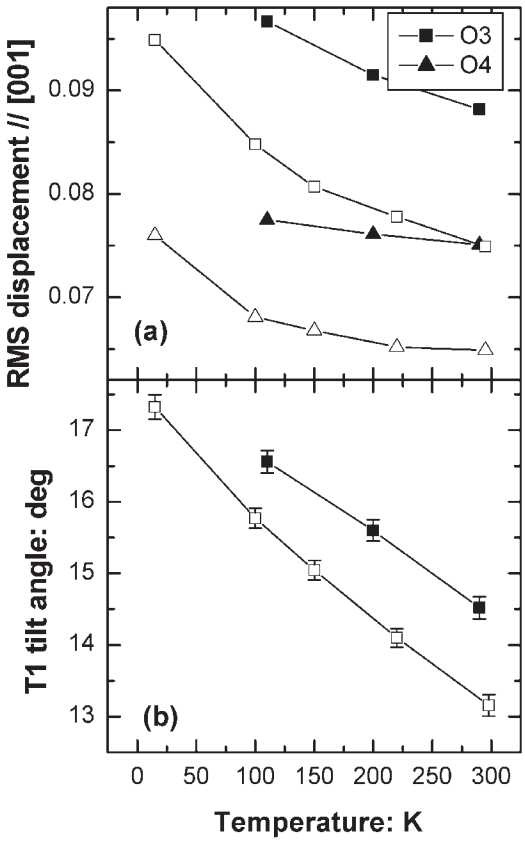

FIG. 4. (a) The variation with temperature of the *rms* displacement of the O3 and O4 oxygen atoms subparallel to [001]. (b) The variation of the tilt angle of the *T*1 and *T*2 tetrahedra with temperature. The solid symbols are for the natural sample, and the open symbols are for the annealed sample. This convention is followed in all subsequent figures. The increases in the magnitude of the displacement ellipsoids and the tilt angle indicate that the refined parameters represent the increase in tilting of essentially rigid tetrahedra as temperature decreases.

DISCUSSION

Our structure refinements of both the natural sample of nepheline and the samples previously annealed to induce K–□ disorder show that as temperature decreases, the average tilts of the *T*1 and *T*2 tetrahedra within the structure increase (Fig. 4b). Further, the tilts are greater in the natural sample than in the annealed sample at the same temperature. At the same time, the intensities of the satellite reflections increase with decreasing temperature, and are stronger and sharper in the natural sample (Fig. 2). We can thus conclude that the intensities of the satellite reflections are correlated with the tilts of the tetrahedra, and thus arise from the modulation of the framework in a rigid-unit mode, as proposed by Hayward *et al*. (2000). The displacement of the O1 oxygen atom from the triad axis, and the *T*1–O1–*T*2 bond angle, are therefore measures of the

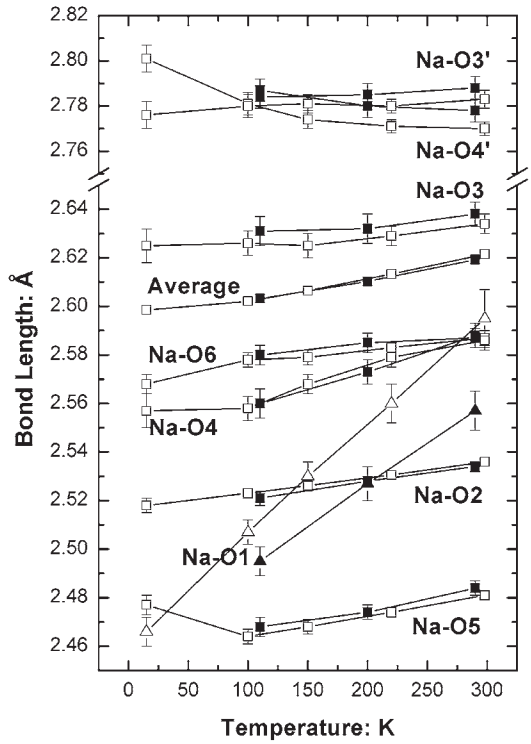

FIG. 5. The variation of Na–O distances in nepheline with temperature.

effective average amplitude of the tilts of the tetrahedra and thus the amplitude of the rigid-unit modulation of the framework. This conclusion is supported by the observation that the displacement of the O1 oxygen atom from the triad axis in nepheline decreases with increasing pressure (Gatta & Angel 2007) as the satellite intensities decrease, and where the satellites were no longer observable, the O1 position refined to the triad axis.

A decrease in the tilts of the *T*1 and *T*2 tetrahedra (equivalent to an increase in the *T*1–O1–*T*2 angle toward 180°) thus represents a decrease in the magnitude of the modulation, as averaged over the coherence length of X-ray diffraction. Such a decrease in the average amplitude of modulation (and thus tilts in the average structure) could arise by two general mechanisms that cannot be distinguished through refinement of the average structure alone. It is possible that the magnitude of the tilts decreases uniformly in a fully coherent way throughout the sample (or at least on the >500 Å length scale). As a second possibility, the coherence length of the modulation may fall below that of X-ray diffraction, while maintaining the amplitude of the local modulation. This would lead to a diminution of the satellite intensities in the same way that the intensities of conventional superlattice reflections arising from ordering decrease when the domain size becomes small, even while the domains themselves remain fully ordered, as in plagioclase (*e.g.*, Kirkpatrick *et al.* 1987, Angel *et al.* 1990). The observation that the satellites are broader in the annealed sample and, in addition, are connected by streaks of diffuse scattering (Fig. 2), suggests that the second mechanism is operational in nepheline.

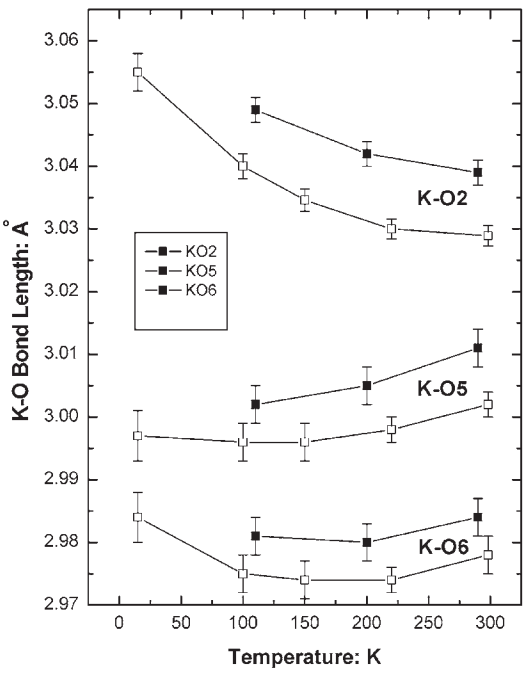

FIG. 6. The variation of K–O bond distances in nepheline with temperature. Note the expansion of the K–O2 distance as temperature is decreased.

Changes in the degree of order of potassium and vacancies in the channels cannot contribute any change to the intensities of the Bragg reflections, because only a single site is involved in the average structure with $P6_3$ symmetry. Therefore, ordering of K and vacancies only contributes to the intensities of the satellite reflections, in agreement with the deductions made from *in situ* measurements of satellite intensities at high temperatures (McConnell 1981). Further, temperature-induced migration of cations *between* the two types of channels that could lead to Na–K exchange is ruled out by the small "free diameters" (Baerlocher *et al.* 2001) of the six-membered rings that provide the only potential path for diffusion between the channels, as confirmed by the results of previous refinements of the structure at elevated temperatures (Foreman & Peacor 1970). Therefore, the changes in the tilts that we see in the average structure upon annealing can only arise from changes in the state of K–□ order in the trigonal channel, through some form of coupling between the atoms in that channel and the framework. The atomic scale mechanism of such a coupling has long been a mystery, as the biggest change in the structure upon introducing K–□ disorder occurs at the O1 site, which is more than 5 Å from center of the nearest trigonal [001] channel (Fig. 3). There is therefore no direct bond between the K in the trigonal channel and the O1 atoms. Neither does the O1 oxygen atom form part of a tetrahedron that has another oxygen atom bonded to the K atom. The coupling must nonetheless involve K–O bonds, as that is the only connection between the K and the framework. Of the three symmetry-independent K–O bonds, K–O5 and K–O6 show a mixed variation with changes in the tilts of the tetrahedra; with decreasing temperature, the bonds shorten as the tilts get larger, whereas they also shorten if the sample is annealed and the tilts get smaller (Fig. 6). In contrast, the K–O2 bonds invariably lengthen if the *T*1,*T*2 tilts get larger, even as temperature is decreased (Figs. 6, 7). Thus the refinements indicate that the K–O2 bond is the immediate mechanism for the coupling between ordering in the trigonal channel and the modulation of the framework. One can further deduce the essentials of the entire mechanism. As K and vacancies are disordered, the average K–O2 bond length becomes shorter. The shortening is accomplished by a shift of the O2 atom position that imposes a rotation on the *T*3 and *T*4 tetrahedra, which opposes the rotation locally required by the framework modulation (Fig. 3), thus reducing either its coherence or magnitude, or

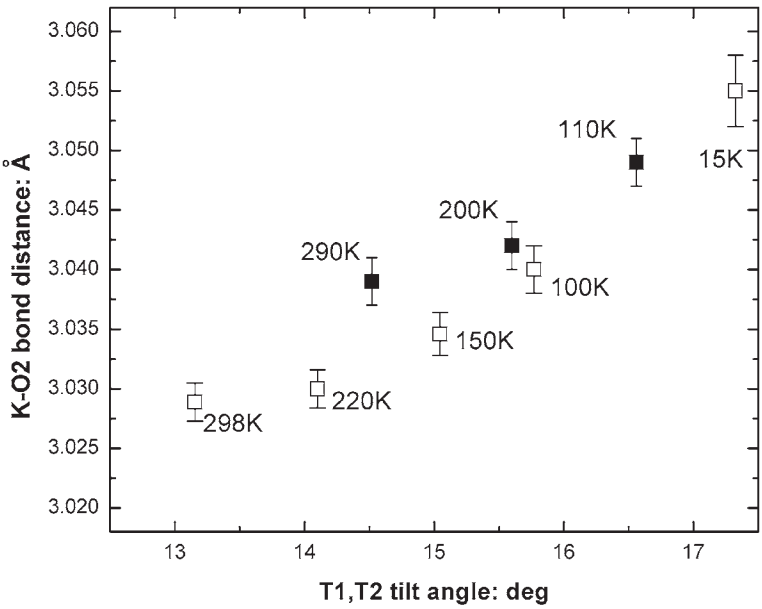

FIG. 7. Variation of K–O2 bond length with the tilt angle of the *T*1 and *T*2 tetrahedra.

more probably both together, and thus decreasing the *T*1 and *T*2 tilts.

The results of the distance-least-squares simulation of the framework of tetrahedra alone seem to support this analysis, although it must be remembered that the simulation is performed in a supercell that can only represent an average of the modulation. Each atomic site except O1 within the average structure becomes three symmetrically distinct sites within the $\sqrt{3}a$, c supercell constrained to the $P6_3$ symmetry. The O1 split site at $^2/_3$ $^1/_3$ z of the average structure becomes a single, fully occupied, unsplit site on a general equivalent position within the supercell. Where constrained to the experimental cell parameters, the DLS simulation in the supercell converges to a structure with a *T*1–O1–*T*2 bond angle of 157° and a displacement of the O1 atom in the same direction as found experimentally. The retention of $P6_3$ symmetry means that there are two symmetrically distinct trigonal channels that contain the K and vacancies. One lies on the 6_3 axis and becomes slightly expanded with respect to the average structure; the "free diameter" is ~2.55 Å compared to ~2.49 Å in the natural material at room temperature. If the K atoms are placed in a position inherited from the average structure, one obtains an average K–O bond length of ~3.10 Å, compared to ~3.01 Å in the average structure. The second channel is strongly ditrigonally distorted and contains two symmetrically distinct sites that alternate along the channel direction (Fig. 1b). The tilts of the rigid tetrahedra result in a slight expansion of one of these sites (<K–O> = 3.07 Å), but significant compression of the other, with the average K–O bond length compressed to ~2.79 Å. The largest and smallest free diameters of this now-elliptical channel are reduced to ~2.41 and ~1.99 Å, respectively. Thus the simulation shows that the shift of the O1 site causes tilts of the tetrahedra that result in significant changes to channels that contain the K and vacancies, even without considering any possible displacements of the K atoms from the channel centers that are allowed by the symmetry of the supercell.

Our results also explain the large range in *T*1–O1–*T*2 angles reported in various refinements of nepheline at room conditions, even though all other bond lengths and angles are essentially identical. Small variations in both the thermal histories of the samples as well as in the proportion of the extra-framework cations will lead to different states of cation order in different crystals. Thus, our sample has a composition that corresponds to the trigonal channel being 80% occupied. This will naturally lead to a pattern of order with a five-fold repeat along [001]. This appears to match the intrinsic wavelength of the rigid-unit modulation (Hayward *et al.* 2000) of the framework. Order of K and vacancies thus leads to an unusually strong modulation and the observed strong intensities of the satellites (McConnell 1962). In other samples with fewer vacancies in the trigonal channels, the state of order will not be as great, and will not match the intrinsic five-fold repeat of the modulation. As a consequence, the amplitude of the

modulation of the framework will be weaker, and the refined tilts of the *T*1 and *T*2 tetrahedra will be less, and the *T*1–O1–*T*2 angles will be larger, as observed.

Acknowledgements

This work was supported by the NSF in form of a grant EAR–0408460 to N.L. Ross and R.J. Angel, the College of Science at Virginia Tech, and an award from the Società Italiana di Mineralogia e Petrologia to G. Diego Gatta. We thank Prof. Desmond McConnell, an anonymous referee and Prof. Robert F. Martin for their comments on the manuscript. This paper is dedicated to the memory of Prof. J.V. Smith, whose work on framework minerals has influenced the research of all of the authors.

References

Angel, R.J., Carpenter, M.A. & Finger, L.W. (1990): Structural variation associated with compositional variation and order–disorder behavior in anorthite-rich feldspars. *Am. Mineral.* **75**, 150-162.

Baerlocher, C., Hepp, A. & Meier, W. (1977): Dls–76, *A Program for the Simulation of Crystal Structures by Geometric Refinement*. Institut für Kristallographie, ETH, Zurich, Switzerland.

Baerlocher, C., Meier, W.M. & Olson, D.H. (2001): *Atlas of Zeolite Framework Types*. Elsevier, Amsterdam, The Netherlands.

Buerger, M.J., Klein, G.E. & Donnay, G. (1954): Determination of the crystal structure of nepheline. *Am. Mineral.* **39**, 805-818.

Dollase, W.A. (1970): Least-squares refinement of the crystal structure of a plutonic nepheline. *Z. Kristallogr.* **132**, 27-44.

Dollase, W.A. & Peacor, D.R. (1971): Si–Al ordering in nephelines. *Contrib. Mineral. Petrol.* **30**, 129-134.

Farrugia, L.J. (1999): Win–GX suite for small-molecule single-crystal crystallography. *J. Appl. Crystallogr.* **32**, 837-838.

Foreman, N. & Peacor, D.R. (1970): Refinement of the nepheline structure at several temperatures. *Z. Kristallogr.* **132**, 45-70.

Gatta, G.D. & Angel, R.J. (2007): Elastic behavior and pressure-induced structural evolution of nepheline: implications for the nature of the modulated superstructure. *Am. Mineral.* **92**, 1446-1455.

Gregorkiewitz, M. (1984): Crystal structure and Al/Si-ordering of a synthetic nepheline. *Bull. Minéral.* **107**, 499-507.

Hahn, T. & Buerger, M.J. (1954): The detailed structure of nepheline, $KNa_3Al_4Si_4O_{16}$. *Z. Kristallogr.* **106**, 308-338.

Hassan, I., Antao, S.M. & Hersi, A.A.M. (2003): Single-crystal XRD, TEM, and thermal studies of the satellite reflections in nepheline. *Can. Mineral.* **41**, 759-783.

Hayward, S.A., Pryde, A.K.A., De Dombal, R.F., Carpenter, M.A. & Dove, M.T. (2000): Rigid unit modes in disordered nepheline: a study of a displacive incommensurate phase transition. *Phys. Chem. Minerals* **27**, 285-290.

Hovis, G.L., Spearing, D.R., Stebbins, J.F., Roux, J. & Clare, A. (1992): X-ray powder diffraction and ^{23}Na, ^{27}Al, ^{29}Si MAS–NMR investigation of nepheline–kalsilite crystalline solutions. *Am. Mineral.* **77**, 19-29.

Kirkpatrick, R.J., Carpenter, M.A., Yang, Wang-Hong & Montez, B. (1987): ^{29}Si magic-angle NMR-spectroscopy of low-temperature ordered plagioclase feldspars. *Nature* **325**, 236-238.

McConnell, J.D.C. (1962): Electron diffraction study of subsidiary maxima of scattered intensity in nepheline. *Mineral. Mag.* **33**, 114-124.

McConnell, J.D.C. (1981): Time–temperature study of the intensity of satellite reflections of nepheline. *Am. Mineral.* **66**, 990-996.

McConnell, J.D.C. (1991): Incommensurate structures. *Phil. Trans., R. Soc. London* **A 334**, 425-437.

Parker, J.M. (1970): *The Fine Structure of Nepheline*. Ph.D. thesis, University of Cambridge, Cambridge, U.K.

Parker, J.M. (1972): The domain structure of nepheline. *Z. Kristallogr.* **136**, 255-272.

Parker, J.M. & McConnell, J.D.C. (1971): Transformation behaviour in the mineral nepheline. *Nature* (*Phys. Sci.*) **234**, 178-179.

Sahama, T.G. (1958): A complex form of natural nepheline from Iivaara, Finland. *Am. Mineral.* **43**, 165-166.

Sheldrick, G.M. (2008): A short history of SHELX. *Acta Crystallogr.* **A 64**, 112-122.

Simmons, W.B. & Peacor, D.R. (1972): Refinement of the crystal structure of a volcanic nepheline. *Am. Mineral.* **57**, 1711-1719.

Smith, J.V. & Sahama, T.G. (1954): Determination of the composition of natural nephelines by an X-ray method. *Mineral. Mag.* **30**, 439-449.

Stebbins, J.F., Murdoch, J.B., Carmichael, I.S.E. & Pines, A. (1986): Defects and short-range order in nepheline group minerals: a silicon-29 nuclear magnetic resonance study. *Phys. Chem. Minerals* **13**, 371-381.

Tait, K.T., Sokolova, E., Hawthorne, F.C. & Khomyakov, A.P. (2003): The crystal chemistry of nepheline. *Can. Mineral.* **41**, 61-70.

Received August 29, 2007, revised manuscript accepted August 31, 2008.